33ND INTERNATIONAL COSMIC RAY CONFERENCE, RIO DE JANEIRO 2013
THE ASTROPARTICLE PHYSICS CONFERENCE

ICRC 2013

Indirect search of dark matter with the ANTARES neutrino telescope

JUAN JOSÉ HERNÁNDEZ–REY[1], GUILLAUME LAMBARD[1] FOR THE ANTARES COLLABORATION.

[1] *IFIC - Instituto de Física Corpuscular (CSIC- Universitat de València), E-46980 Paterna, Spain*

Juan.J.Hernandez@ific.uv.es

Abstract: The results of a search for high-energy neutrinos coming from the direction of the Sun using the data recorded by the ANTARES neutrino telescope during 2007 and 2008 are presented. The number of neutrinos observed is found to be compatible with background expectations and upper limits for the spin-dependent and spin-independent WIMP-proton cross-sections are derived and compared to predictions of the CMSSM. These limits are comparable to those obtained by other neutrino telescopes and are more stringent than those obtained by direct search experiments for the spin-dependent WIMP-proton cross-section assuming the self-annihilation proceeds through hard channels, i.e. via W^+W^- and $\tau^+\tau^-$.

Keywords: dark matter, WIMPs, neutralino, SUSY, neutrino telescopes, ANTARES

1 Introduction

The existence of dark matter, i.e. non-baryonic matter that does not interact electromagnetically, has been educed from a variety of gravitational effects. The rotation curves of galaxies and galaxy clusters and the observations of weak lensing point to the existence of dark matter. It is also required to understand the features of the cosmic microwave background and the large scale structure formation within our present accepted models of the evolution of the Universe [1].

One hypothesis is that dark matter is formed by weakly interacting massive particles (WIMPs), candidates for which are copiously provided by different extensions of the Standard Model, in particular those based on Supersymmetry (SUSY). Within SUSY models the lightest neutralino is one of the favoured candidates for dark matter WIMP.

WIMPs can be captured in massive astrophysical objects, like the Sun, where they can self-annihilate giving rise to high-energy neutrinos. Neutrino telescopes are well suited to look for such a signal coming from sources like the Sun or the centre of the Galaxy. This type of indirect search complements direct searches and has a variety of advantages compared to others. For the case of the Sun, for instance, such a WIMPigenic neutrino flux depends only mildly on the WIMP velocity distribution. On the other hand, it has a strong dependence on the WIMP-proton cross-section, in particular the part that involves spin, making it very sensitive to this important magnitude. Moreover, unlike other indirect searches (e.g. using gamma-rays or positrons) a signal would be very clean, since it is very difficult to imagine astrophysical processes that would produce high-energy neutrinos coming from the Sun and those which are possible can only yield negligible fluxes.

2 ANTARES

ANTARES is an undersea neutrino telescope located in the Mediterranean Sea, 40 km offshore from Toulon (France) [2]. The telescope consists of 12 detection lines anchored to the seabed at 2475 m depth. Each line has 25 storeys. A standard storey includes three optical modules (OMs) [3] each housing a 10-inch photomultiplier [4] and a local control module that contains the electronics [5, 6]. The OMs are directed 45° downwards so as to optimise their acceptance to upgoing light and to avoid the effect of sedimentation and biofouling [7]. The length of a line is 450 m and the horizontal distance between neighbouring lines is 60-75 m. In one of the lines, the upper storeys put up a test system for acoustic neutrino detection [8]. Other acoustic devices are installed in an additional line that contains instrumentation aimed at measuring environmental parameters [9]. The location of the active components of the lines is known better than 10 cm by a combination of tiltmeters and compasses in each storey and a series of acoustic transceivers in certain storeys along the line and surrounding the telescope [10]. A common time reference is maintained in the full detector by means of a 25 MHz clock signal broadcast from shore. The time offsets of the individual optical modules are determined in dedicated calibration facilities onshore and regularly monitored in situ, and corrected if needed, by means of optical beacons distributed throughout the lines and which emit short light pulses through the water [11]. This allows to reach a sub-nanosecond accuracy on the relative timing [12].

The first 5 lines of the detector were operational in 2007 and the full detector with 12 lines was completed in May 2008.

3 Event selection

The search presented here uses the data taken during 2007 and 2008 by the ANTARES neutrino telescope. Good detector and environmental conditions, in particular a low level of bioluminescent light, are required for a run to be kept for further analysis. For that period, a total of 2693 runs are found to have the appropiate conditions. This corresponds to a livetime of 134.6, 38.0, 39.0 and 83.0 days for the periods in which the dectector consisted of 5, 9, 10 and 12 lines, respectively.

The muon tracks are reconstructed from the position and time of the hits of the Cherenkov photons in the OMs. The reconstruction algorithm is based on the minimisation of a χ^2-like quality parameter, Q, which uses the difference between the expected and measured times of the detected photons plus a correction term that takes into account

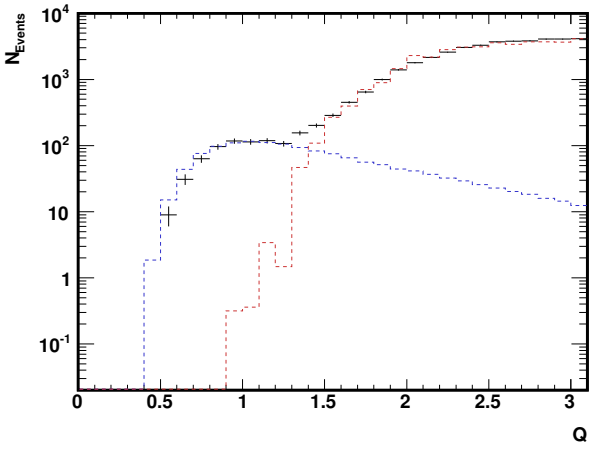

Figure 1: Number of events as a function of the quality parameter of the track fit, Q. The blue and red dashed lines correspond to the atmospheric neutrino and muon events, respectively, according to simulation, and the black crosses are the 2007-2008 data.

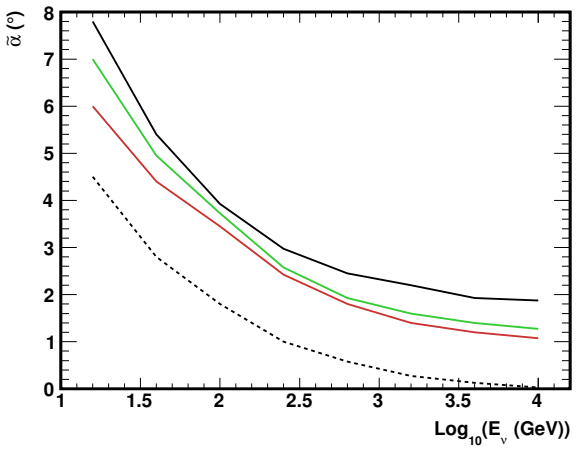

Figure 2: Angular resolution for upgoing neutrinos for the detector configuration with 5 (black), 9 (green) and 10 and 12 (red) lines. The black dashed line is the resolution due solely to the angle between the muon and the neutrino at the interaction vertex.

the effect of light absorption [13]. The distribution of the number of events as a function of this quality parameter, Q, shows a good agreement between data and simulated events, as can be seen in figure 1. The angular resolution provided by this algorithm for upgoing neutrinos depends on the configuration of the detector and of the neutrino energy. In figure 2, the angular resolution for upgoing neutrinos as a function of the neutrino energy is shown for the different detector configurations.

The fit of the muon track is required to use a number of hits greater than five in at least two lines. This yields a non-degenerate 5-parameter fit that provides a good angular resolution. Only events that go upwards, according to the fitted angle, are kept in order to reject most of the atmospheric muon background. The quality parameter of the track, Q, and its angular distance to the Sun, Ψ, are then used to further reduce the background. They are chosen so as to optimise the model rejection factor [14]. For each WIMP mass and each annihilation channel, the selected values, Q_{cut} and Ψ_{cut}, are specifically those that minimise the average 90% confidence level (CL) upper limit on the $\nu_\mu + \bar{\nu}_\mu$ flux, $\overline{\Phi}_{\nu_\mu+\bar{\nu}_\mu}$, defined as:

$$\overline{\Phi}_{\nu_\mu+\bar{\nu}_\mu} = \frac{\bar{\mu}^{90\%}}{\sum_i \bar{A}^i_{eff}(M_{WIMP}) \times T^i_{eff}}, \qquad (1)$$

where the index i denotes the periods with different detector configurations (5, 9, 10 and 12 detection lines), $\bar{\mu}^{90\%}$ is the average upper limit of the background at 90% CL computed using a Poisson distribution with the Feldman-Cousins prescription [15], T^i_{eff} is the livetime for each detector configuration and $\bar{A}^i_{eff}(M_{WIMP})$ is the effective area averaged over the neutrino energy.

To perform this optimisation, simulated events both for the signal and the background were generated. Downgoing atmospheric muons were simulated using Corsika [16] and upgoing atmospheric neutrinos using the Bartol flux [17]. A possible background coming from the interaction of cosmic rays with the Sun's corona was neglected, since it was found to be less than 0.4% of the total atmospheric background in the Sun's direction.

The signal was simulated assuming that the high-energy neutrinos from the Sun were produced by the annihilation of neutralinos. The flux of neutrinos as a function of their energy arriving at the Earth's surface from the Sun's core was computed using the software package WimpSim [18] without assuming any concrete model. The neutrinos resulting from the neutralino self-annihilation channels to $q\bar{q}$, $l\bar{l}$, W^+W^-, ZZ, Higgs doublets $\phi\phi^*$ and $\nu\bar{\nu}$ were simulated for 17 different WIMP masses ranging from 10 GeV to 10 TeV. Three main self-annihilation channels were chosen as benchmarks for the lightest neutralino, $\tilde{\chi}^0_1$, namely: a soft neutrino channel, $\tilde{\chi}^0_1\tilde{\chi}^0_1 \to b\bar{b}$, and two hard neutrino channels, $\tilde{\chi}^0_1\tilde{\chi}^0_1 \to W^+W^-$ and $\tilde{\chi}^0_1\tilde{\chi}^0_1 \to \tau^+\tau^-$. A 100% branching ratio was assumed for all of them in order to explore the widest theoretical parameter space. Oscillations among the three neutrino flavours (both in the Sun and during their flight to Earth) were taken into account, as well as ν absorption and τ lepton regeneration in the Sun's medium.

The optimisation procedure gave a stable value of 1.4 for Q_{cut}, independently of the cut on the angle to the Sun's direction. The optimised values for the latter, Ψ_{cut}, were typically between 3.5° and 5.5°. The extreme upper and lower values for this cut, namely 8.4° and 3.2°, occurred, respectively, for low mass in the soft-channel (M_{WIMP}= 50 GeV and $b\bar{b}$) and for high masses in the hard channels ($M_{WIMP} > 1$ TeV and W^+W^-, $\tau^+\tau^-$), as expected.

4 Results

After unblinding, a total of 27 events are found within a 20° angular separation from the Sun's direction. In figure 3 the distribution of the angular distance for the selected event tracks is shown. The triangles are the data with the one sigma statistical uncertainty and the straight line is the expected background obtained scrambling the data in right ascension. No significant excess is found.

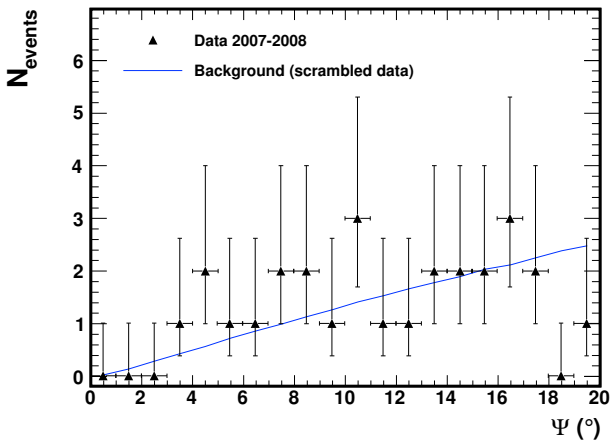

Figure 3: Number of events as a function of the angle between the track and the Sun's direction. The straight line is the expected background as obtained scrambling real data. The triangles are the data.

Using the values for the cuts obtained in the optimisation procedure, 90% CL limits on the $\nu_\mu + \bar{\nu}_\mu$ flux, $\Phi_{\nu_\mu+\bar{\nu}_\mu}$, can be extracted from the data according to Equation 1, where now $\mu^{90\%}$ is not the average but the actual 90% CL limit on the number of observed events. The limits on the muon flux are calculated using a conversion factor between the neutrino and the muon fluxes computed using the package DarkSUSY [19]. Figure 4 shows the 90% CL muon flux limits, Φ_μ, for the channels $b\bar{b}$, W^+W^- and $\tau^+\tau^-$. The latest results from Baksan [20], Super-Kamiokande [21] and IceCube-79 [22] are also shown for comparison.

CMSSM Parameter Range
$50\ \text{GeV} < m_0 < 4\ \text{TeV}$
$500\ \text{GeV} < m_{1/2} < 2.5\ \text{TeV}$
$5 < \tan\beta < 62$
$-5\ \text{TeV} < A_0 < 5\ \text{TeV}$
$\text{sgn}(\mu) > 0$

Table 1: Range of parameters scanned for the CMSSM model. m_0 and $m_{1/2}$ are the common scalar and gaugino masses, respectively; $\tan\beta$ is the ratio of vevs of the Higgs field; A_0 is the common trilinear coupling and $\text{sgn}(\mu)$ the sign of the Higgs mixing.

Limits on the spin-dependent (SD) and spin-independent (SI) WIMP-proton scattering cross-sections –when one or the other is dominant– can also be obtained. To this end, the following assumptions are made. First, equilibrium between the WIMP capture and self-annihilation rates in the Sun is assumed. Secondly, the Sun is considered to be free in the galactic halo. Thirdly, a local dark matter density of 0.3 GeV cm^{-3} and a Maxwellian velocity distribution of the WIMP with a dispersion of 270 km s^{-1} are used. Finally, it is assumed that no additional dark matter disk that could enhance the local dark matter density exists.

The 90% CL limits for the SD, $\sigma_{p,SD}$, and SI, $\sigma_{p,SI}$, WIMP-proton cross-sections extracted from the self-annihilation channels to $b\bar{b}$, W^+W^- and $\tau^+\tau^-$ are presented in Figure 5. Systematic uncertainties were included in the evaluation of the limits following the approach described in reference [27]. The total systematic uncertainty on the detector efficiency is around 20% and comes essentially from the uncertainties on the average quantum efficiency and the angular acceptance of the PMTs and the sea water absorption length (a 10% uncertainty for each one). This systematic uncertainty worsens the upper limit between 3% and 6%, depending on the WIMP mass.

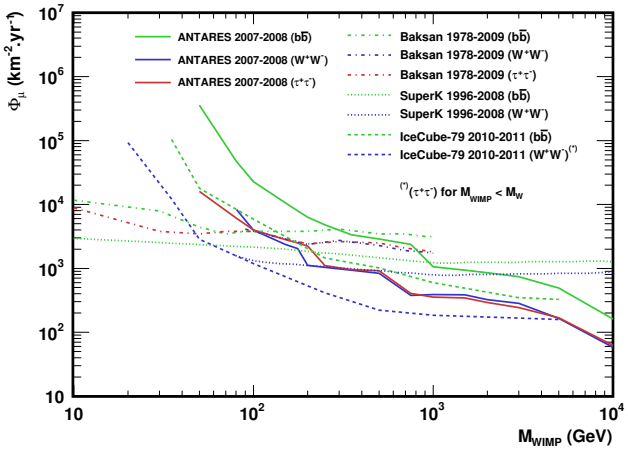

Figure 4: 90% CL upper limit on the muon flux as a function of the WIMP mass for the neutralino self-annihilation channels to $b\bar{b}$ (green), W^+W^- (blue) and $\tau^+\tau^-$ (red). The results from Baksan 1978 – 2009 [20] (dash-dotted lines), Super-Kamiokande 1996 – 2008 [21] (dotted lines) and IceCube-79 2010 – 2011 [22] (dashed lines) are also shown.

Also shown in Figure 5 are the latest results from Baksan [20], Super-Kamiokande [21] and IceCube-79 [22] as well as the limits from the direct search experiments SIMPLE [23], COUPP [24] and XENON100 [25].

The allowed values from the CMSSM model according to the results from an adaptative grid scan performed with DarkSUSY are also shown. The parameters of this model are moved within the ranges indicated in Table 1. All the limits are computed with a muon energy threshold at $E_\mu = 1$ GeV. The shaded regions show a grid scan of the model parameter space taking into account the latest constraints for various observables from accelerator-based experiments and in particular the results on the Higgs boson mass from ATLAS and CMS, $M_h = 125 \pm 2$ GeV [26]. A relatively loose constraint on the neutralino relic density $0 < \Omega_{CDM}h^2 < 0.1232$ is used to take into account the possible existence of other types of dark matter particles.

Since the capture rate of WIMPs in the core of the Sun depends very much on the SD WIMP-proton cross-section, the neutrino flux coming from WIMP annihilation strongly depends on it. This makes this type of indirect search very competitive for this magnitude. This is not the case for the SI WIMP-proton cross-section, where the limits coming from direct search experiments like XENON100 are better thanks to the composition of their target materials.

5 Conclusions

An indirect search for dark matter towards the Sun has been carried out using the first two years of data recorded by

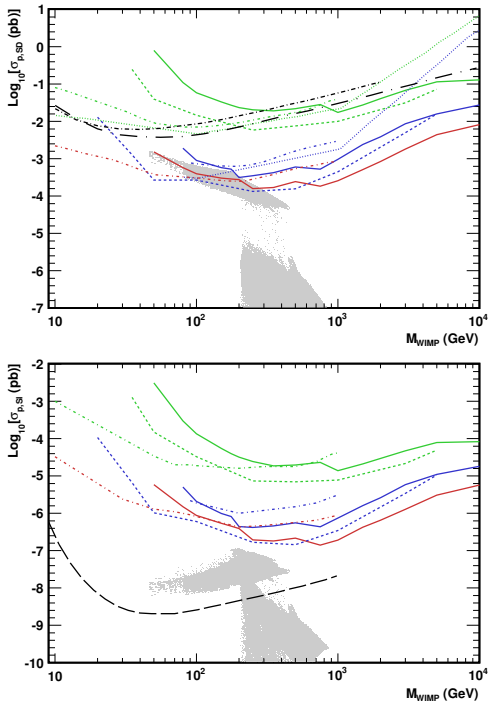

Figure 5: 90% CL upper limits on the SD and SI WIMP-proton cross-sections (upper and lower plots, respectively) as a function of the WIMP mass, for the three self-annihilation channels: $b\bar{b}$ (green), W^+W^- (blue) and $\tau^+\tau^-$ (red), for ANTARES 2007-2008 (solid lines) compared to the results of other indirect search experiments: Baksan 1978 – 2009 [20] (dash-dotted lines), Super-Kamiokande 1996 – 2008 [21] (dotted lines) and IceCube-79 2010 – 2011 [22] (dashed lines) and the result of the most stringent direct search experiments (black): SIMPLE 2004 – 2011 [23] (short dot-dashed line in upper plot), COUPP 2010 – 2011 [24] (long dot-dashed line in upper plot) and XENON100 2011 – 2012 [25] (dashed line in lower plot). The results of a grid scan of the CMSSM are included (grey shaded areas) for the sake of comparison.

the ANTARES neutrino telescope. The number of neutrino events coming from the Sun's direction is compatible with the expectation from the atmospheric backgrounds. The derived limits are comparable to those obtained by other neutrino observatories and are more stringent than those obtained by direct search experiments for the spin-dependent WIMP-proton cross-section. The present ANTARES limits start to constraint the parameter space of the CMSSM model.

Acknowledgment: This work was supported by the Spanish Ministry of Science and Innovation and the Generalitat Valenciana under grants: FPA2009-13983-C02-01, FPA2012-37528-C02-01, PROMETEO/2009/026 and the Consolider MultiDark, CSD 2009-00064

References

[1] G. Bertone, D. Hooper, J. Silk, Phys. Rept., 2005, **405**: pp. 279-390.
[2] M. Ageron et al., ANTARES Collaboration, *ANTARES: the first undersea neutrino telescope*, Nucl. Inst. and Meth. in Phys. Res. A **656** (2011) 11-38.
[3] P. Amram, ANTARES Collaboration, *The ANTARES optical module*, Nucl. Inst. and Meth. in Phys. Res. A **484** (2002) 369.
[4] J.A. Aguilar et al., ANTARES Collaboration, Nucl. Inst. and Meth. in Phys. Res. A **555** (2005) 132.
[5] J.A. Aguilar et al., ANTARES Collaboration, Nucl. Inst. and Meth. in Phys. Res. A **622** (2010) 59.
[6] J.A. Aguilar et al., ANTARES Collaboration, Nucl. Inst. and Meth. in Phys. Res. A **570** (2007) 107.
[7] P. Amram, ANTARES Collaboration, Astropart. Phys. **19** (2003) 253.
[8] J.A. Aguilar et al., ANTARES Collaboration, Nucl. Inst. and Meth. in Phys. Res. A **626-627** (2011) 128.
[9] J.A. Aguilar et al., ANTARES Collaboration, Astropart. Phys. **26** (2006) 314.
[10] S. Adrián-Martínez et al., ANTARES Collaboration, JINST **7** (2012) T08002.
[11] M. Ageron et al., ANTARES Collaboration, Nucl. Inst. and Meth. in Phys. Res. A **578** (2007) 498.
[12] J.A. Aguilar et al., ANTARES Collaboration, Astropart. Phys. **34** (2011) 539.
[13] J.A. Aguilar et al., Astropart. Phys. **34** (2011) 652.
[14] G.C. Hill, K. Rawlins, Astropart. Phys. **19** (2003) 393-402.
[15] G.J. Feldman, R.D. Cousins, Phys. Rev. **D 57** (1998) 3873-3889.
[16] D. Heck et al., Report FZKA 6019 (1998), Forschungszentrum Karlsruhe; D. Heck and J. Knapp, Report FZKA 6097 (1998), Forschungszentrum Karlsruhe.
[17] G. Barr et al., Phys. Rev. D **39**, 3532 (1989); V. Agrawal et al., Phys. Rev. D **53**, 1314 (1996).
[18] J. Edsjö, http://www.physto.se/ edsjo/wimpsim/.
[19] P. Gondolo et al., J. Cosm. and Astropart. Phys., JCAP07, 008 (2004).
[20] M.M. Boliev et al., Baksan Collaboration, [astro-ph/1301.1138].
[21] T. Tanaka et al., Super-Kamiokande Collaboration, Astrophys. J. **742**, 78 (2011).
[22] M.G. Aartsen et al., IceCube Collaboration,Phys. Rev. Lett. 110, (2013) 131302.
[23] M. Felizardo et al., SIMPLE Collaboration, Phys. Rev. Lett. **108** (2012) 201302.
[24] E. Behnke et al., COUPP Collaboration, Phys. Rev. D **86** (2012) 052001.
[25] E. Aprile et al., XENON Collaboration, [astro-ph/1207.5988].
[26] O. Buchmueller et al., [hep-ph/1207.7315].
[27] F. Tegenfeldt, J. Conrad, Nucl. Inst. and Meth. in Phys. Res. A **539** (2005) 407-413; J. Conrad et al., Phys. Rev. D **67**, 012002 (2003); J. Conrad, [astro-ph/0612082].